



SHEBA

European Geosciences Union, General Assembly 2012

Session: NP6.3/AS2.4 Turbulence in the Atmosphere



Upper limit of applicability of the local similarity theory in the stable atmospheric boundary layer

Andrey A. Grachev^{1,2}, Edgar L Andreas³, Christopher W. Fairall²,
Peter S. Guest⁴, and P. Ola G. Persson^{1,2}

¹ *Cooperative Institute for Research in Environmental Sciences, University of Colorado, Boulder, Colorado, USA*

² *NOAA Earth System Research Laboratory, Boulder, Colorado, USA*

³ *NorthWest Research Associates, Inc., Lebanon, New Hampshire, USA*

⁴ *Naval Postgraduate School, Monterey, California, USA*

EGU2012-3256

Manuscript is available at <http://arxiv.org/abs/1202.5066>



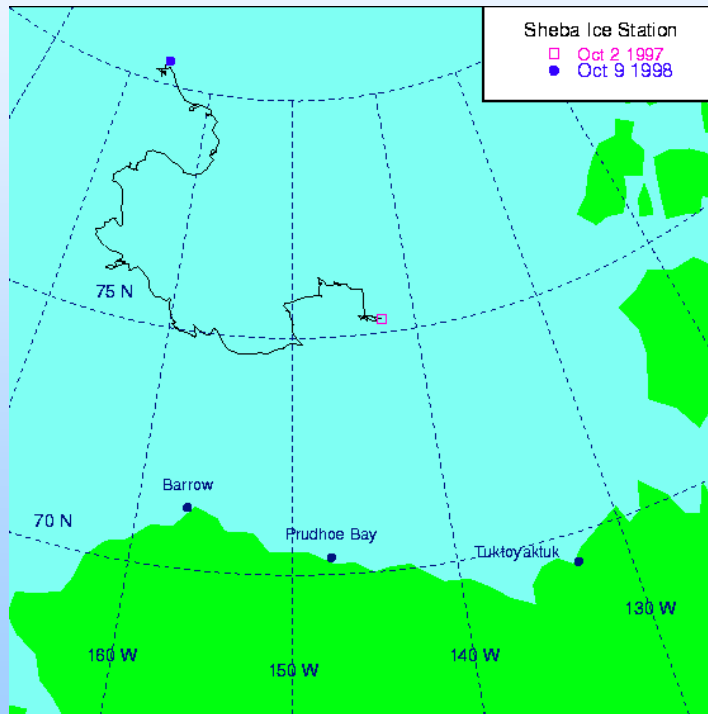
SHEBA

SHEBA Site

Surface Heat Budget of the Arctic Ocean Experiment (SHEBA)



- The main SHEBA ice camp was deployed on the ice in the vicinity of the Canadian Coast Guard ice breaker *Des Groseilliers*, which was frozen into the Arctic ice pack north of Alaska from October 1997 to October 1998.
- During this period, the ice breaker drifted more than 1400 km in the Beaufort and Chukchi Seas, with coordinates varying from approximately 74° N and 144° W to 81° N and 166° W.



The SHEBA ice station drift from October 2, 1997 until October 9, 1998.

The SHEBA ice camp and the *Des Groseilliers*

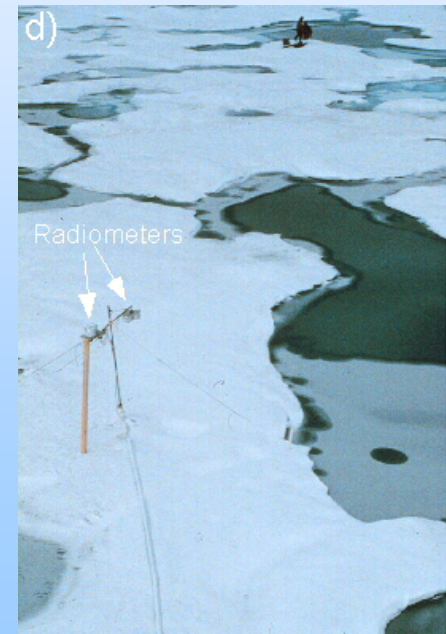
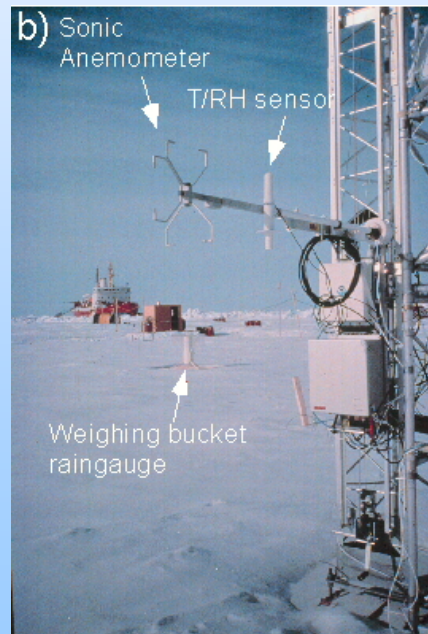


SHEBA

ASFG Instrumentation



- The Atmospheric Surface Flux Group (ASFG) deployed a 20-m main micrometeorological tower, two short masts, and several other instruments on the surface located 280 – 350 m from the *Des Groseilliers* at the far edge of the main ice camp.
- Turbulent and mean meteorological data were collected at five levels, nominally 2.2, 3.2, 5.1, 8.9, and 18.2 m (or 14 m during most of the winter).
- Each level had a Vaisälä HMP-235 temperature/relative humidity probe (T/RH) and identical ATI three-axis sonic anemometers/thermometers (resolution: wind speed 0.01 m/sec; sonic temperature 0.01°C).
- An Ophir fast infrared hygrometer was mounted on a 3-m boom at an intermediate level just below level 4 (8.1 m above ice).





SHEBA

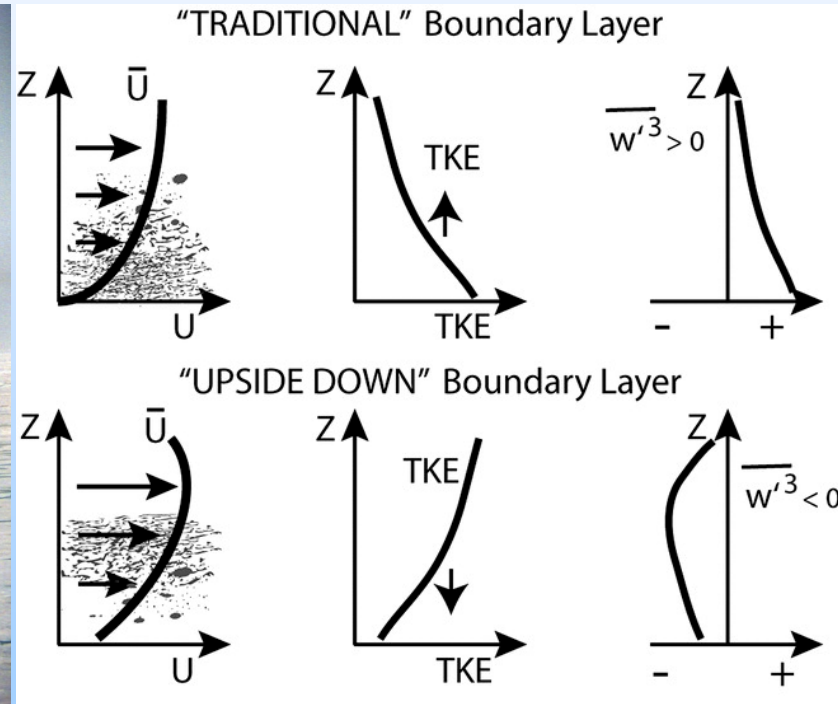
Traditional SBL



- The SHEBA site was located on Arctic pack ice, which had no large-scale slopes or heterogeneities; the site was a few hundred kilometers from land and thus provided almost unlimited and extremely uniform fetch. For these reasons, the SHEBA flux data are not generally contaminated by drainage (katabatic), strong local advective flows, or orographically generated gravity waves.
- Thus the SBL observed most often during SHEBA can be characterized as a traditional SBL layer.



The SHEBA ice camp and C-130



Schematic of structure of (top) traditional boundary layer versus (bottom) upside-down boundary layer (Banta et al (2006) JAS v.63(11) Fig.1)



SHEBA

Monin-Obukhov similarity theory

Obukhov (1946), Monin and Obukhov (1954), Nieuwstadt (1984)



• Monin – Obukhov stability parameter: $\zeta \equiv z / L$ • Obukhov length: $L = - \frac{u_*^3 T_v}{\kappa g < w' T_v' >}$

• Non-dimensional velocity and temperature gradients: $\varphi_m(\zeta) = \frac{\kappa z}{u_*} \frac{dU}{dz}, \quad \varphi_h(\zeta) = \frac{\kappa z}{T_*} \frac{d\theta}{dz}$

• Non-dimensional standard deviations: $\varphi_\alpha(\zeta) = \frac{\sigma_\alpha}{u_*}, \quad \varphi_\theta(\zeta) = \frac{\sigma_\theta}{\theta_*} \quad (\alpha = u, v, w)$

• Gradient Richardson number: $Ri = \frac{g}{T_v} \frac{d\theta_v / dz}{(dU / dz)^2} = \frac{(z / L) \varphi_h}{\varphi_m^2}$

• Flux Richardson number: $Rf = \frac{g}{T_v} \frac{< w' T_v' >}{< u' w' > (dU / dz)} \equiv \frac{z / L}{\varphi_m}$

• Turbulent Prandtl number: $Pr_t = \nu_t / k_t \equiv \varphi_h / \varphi_m \equiv Ri / Rf$

Local z-less stratification

Wyngaard and Coté (1972) and Wyngaard (1973)



- In very stable case MOST predicts that z ceases to be a scaling parameter:

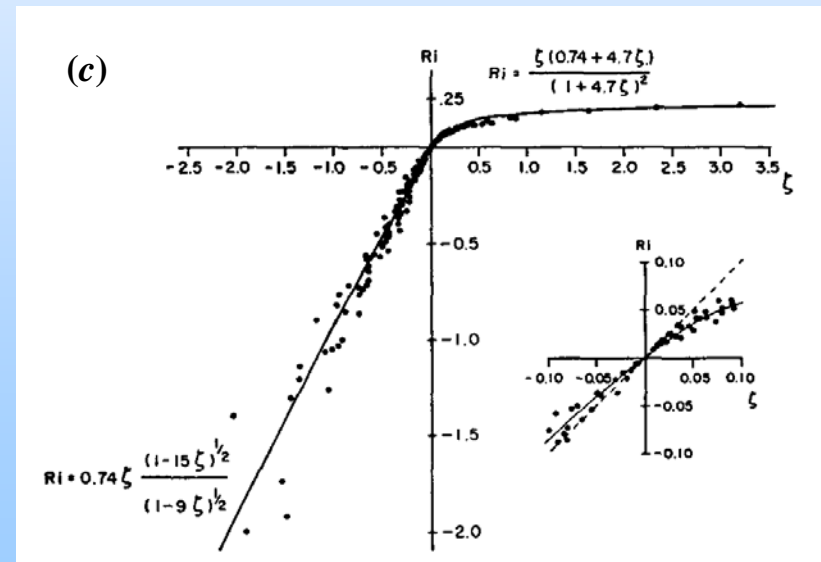
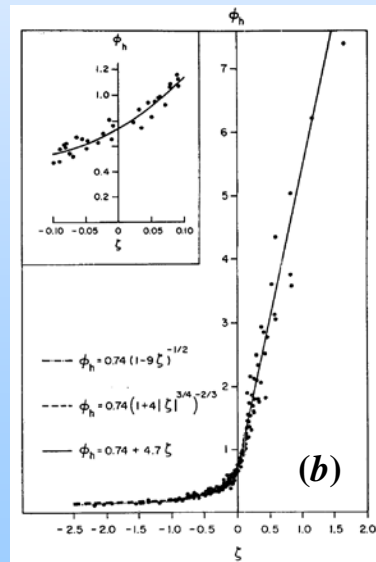
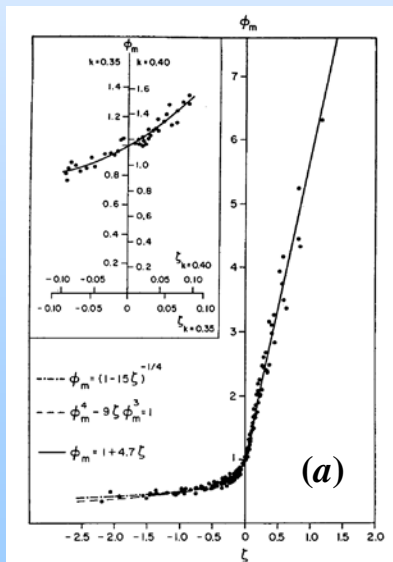
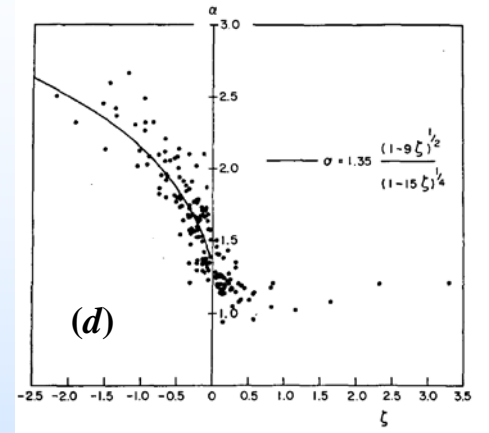
$$\varphi_m(\zeta) = \beta_m \zeta$$

$$\varphi_h(\zeta) = \beta_h \zeta$$

- A simple linear interpolation between neutral and z-less cases :

$$\varphi_m(\zeta) = 1 + \beta_m \zeta$$

$$\varphi_h(\zeta) = 1 + \beta_h \zeta$$



Plots of (a) φ_m , (b) φ_h , (c) Ri , (d) $1/Pr_t$ versus $\zeta = z/L$ from Kansas (1968) experiment (Businger *et al.* (1971) *JAS* v. 28(2), 181–189)

Turbulence spectra and cospectra in the SBL

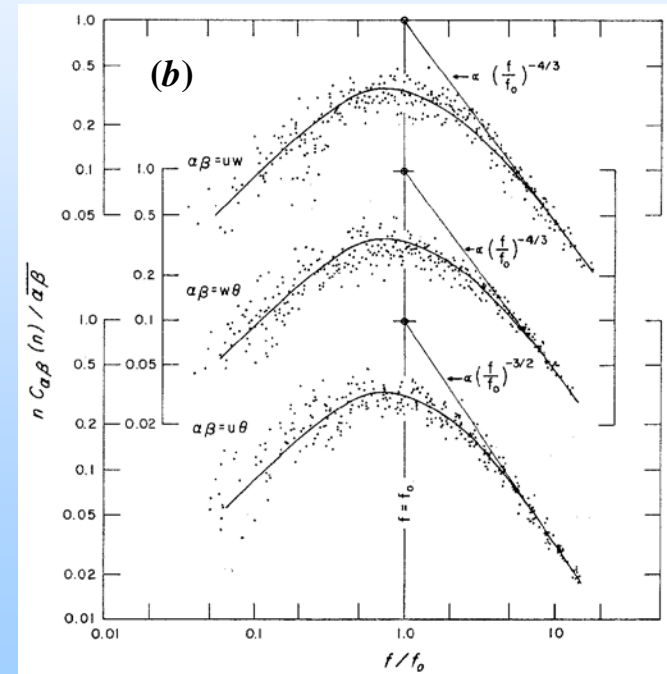
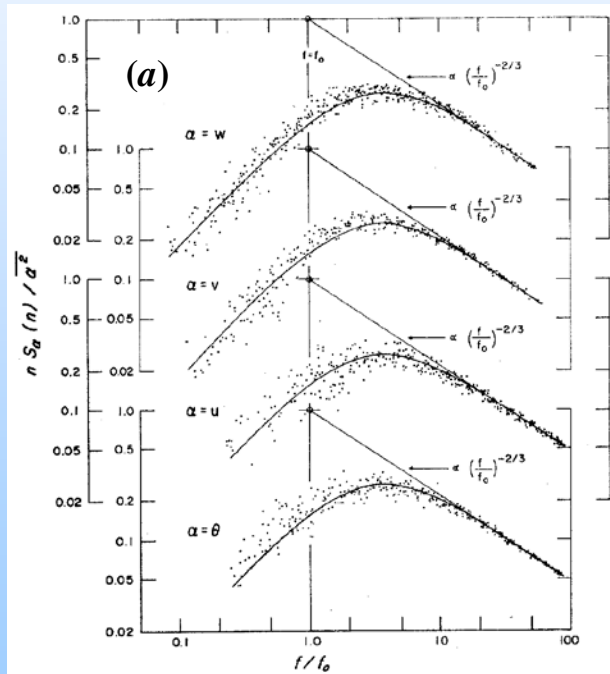
Kaimal et al. (1972), Kaimal (1973), Caughey (1977)



- Observations in the SBL have shown that properly normalized spectra and cospectra can be represented by a series of universal curves based on the Monin-Obukhov scaling:

$$\frac{n \cdot S_{\alpha}(n)}{\sigma_{\alpha}^2} = \frac{0.164 \cdot f / f_0}{1 + 0.164 \cdot (f / f_0)^{5/3}} \quad \alpha = u, v, w, \theta$$

$$\frac{n \cdot C_{\alpha\beta}(n)}{\langle \alpha'w' \rangle} = \frac{0.88 \cdot f / f_0}{1 + 1.5 \cdot (f / f_0)^{2.1}} \quad \alpha = u, \theta$$



Normalized (a) spectra of w , v , u , θ and (b) cospectra of uw , $w\theta$, and $u\theta$ plotted versus f/f_0 based on the Kansas (1968) data (Kaimal et al. (1972) *Q. J. Roy. Meteorol. Soc.*, v.98(417), 563–589).



SHEBA

Local z-less scaling was questioned

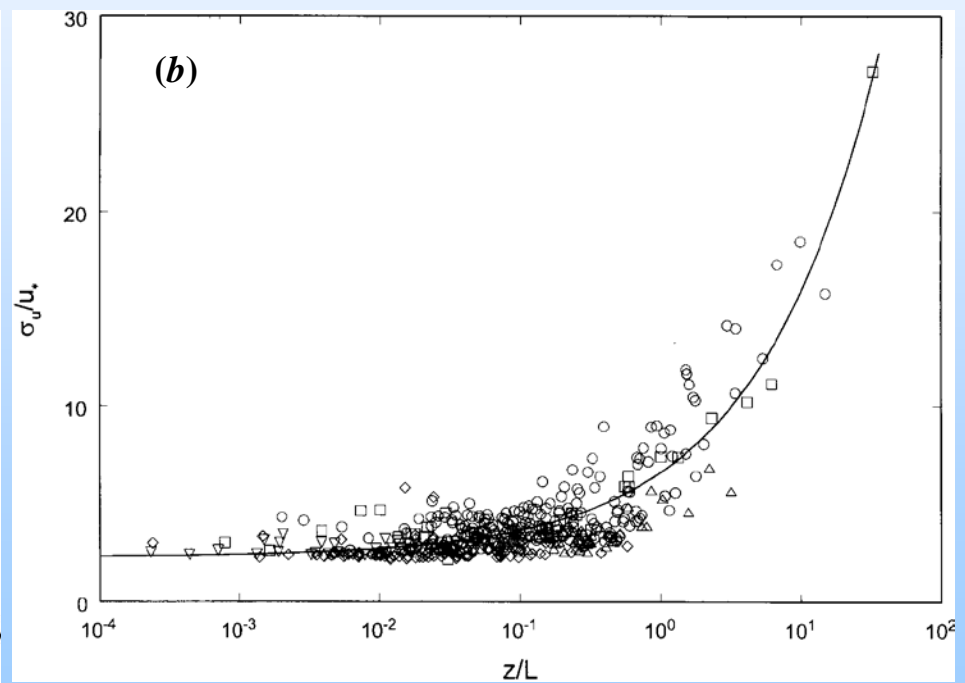
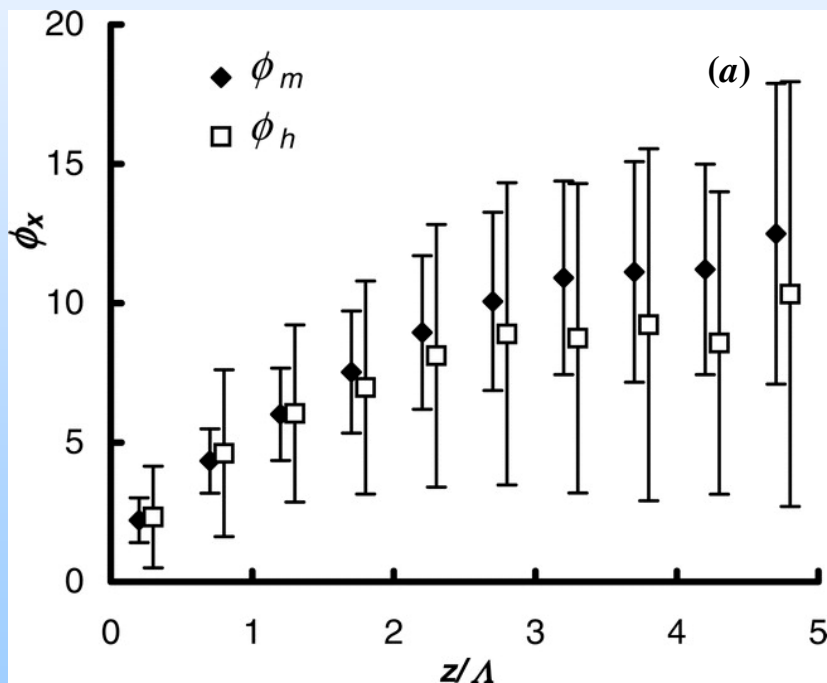
Current extensive datasets



- Local z-less scaling has been brought into question by recent measurements:

Forrer and Rotach (1997)
Howell and Sun (1999)
Yagüe *et al.* (2001, 2006)
Pahlow *et al.* (2001)

Klipp and Mahrt (2004)
Cheng and Brutsaert (2005)
Baas *et al.* (2006)
Grachev *et al.* (2005, 2007)

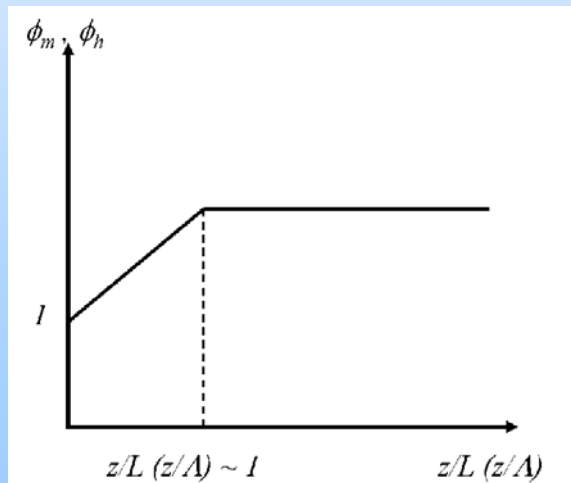


Plots of (a) ϕ_m & ϕ_h versus $\zeta = z/L$ from CASES-1999 experiment (Baas *et al.* (2006) *J. Atmos. Sci.*, 63(11), 3045–3054) and (b) σ_y/u_* versus $\zeta = z/L$ (Pahlow *et al.* (2001) *Boundary-Layer Meteorol.* 99(2), 225–248)

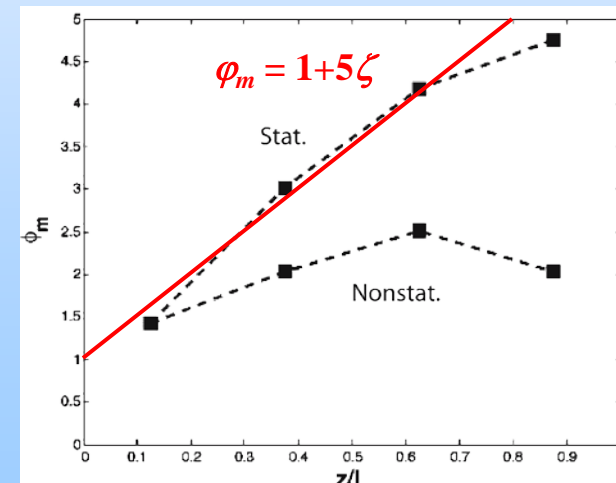
Saving the z-less concept



- Basu *et al.* (2006) revisited the data used by Pahlow *et al.* (2001) and applied rigorous quality control to this and some other datasets to remove non-turbulent effects. Their analysis supported the validity of z-less stratification for σ_w/u_* .
- Mahrt (2007) analyzed extensive eddy-correlation datasets to examine the influence of non-stationarity of the mean flow on the flux-gradient relationships for $\zeta < 1$. However, even for stationary cases, the function $\phi_m(\zeta)$ increases more slowly than the linear prediction in the range $0.6 < \zeta < 1$.
- Hong *et al.* (2010) nevertheless supported the validity of z-less stratification only up to $\zeta \sim 0.5$ by applying the Hilbert-Huang transform to separate turbulent signals from non-turbulent motions.
- These contradictory results indicate that the validity of z-less stratification is still an open question that requires further clarification.



Sketch of ϕ_m & ϕ_h versus $\zeta = z/L$ based on the current data revealing the level-off of ϕ_m & ϕ_h (Hong (2010) *APJAS* v. 46(1))



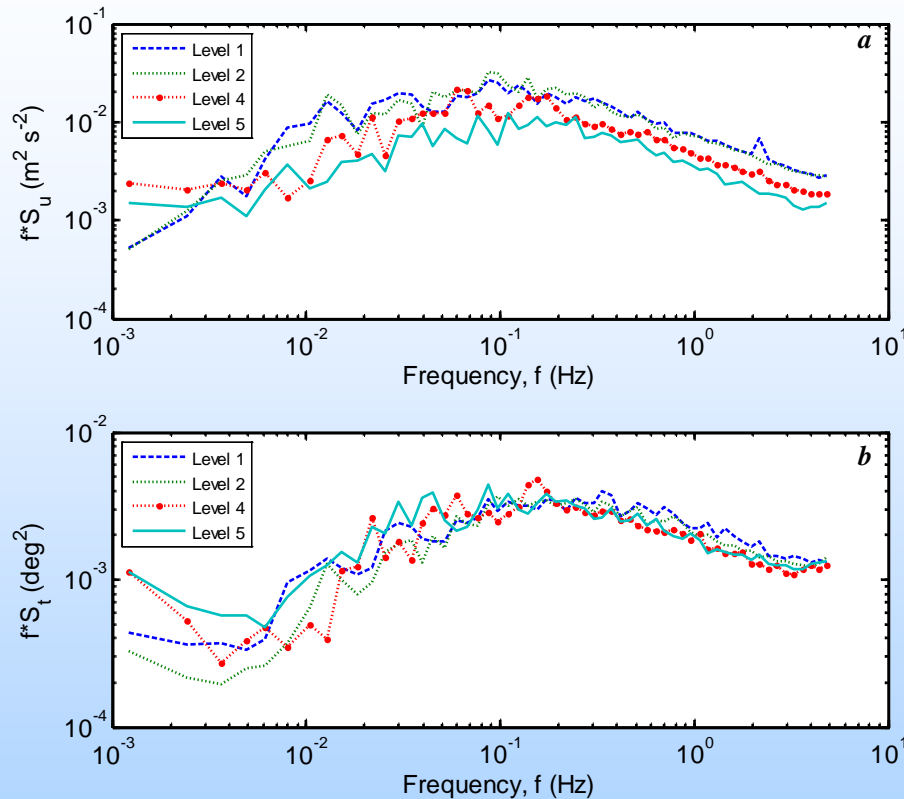
Bin-averaged values of ϕ_m versus $\zeta = z/L$ for stationary and non-stationary cases (Mahrt (2007) *BLM* 125(2), 245–264)



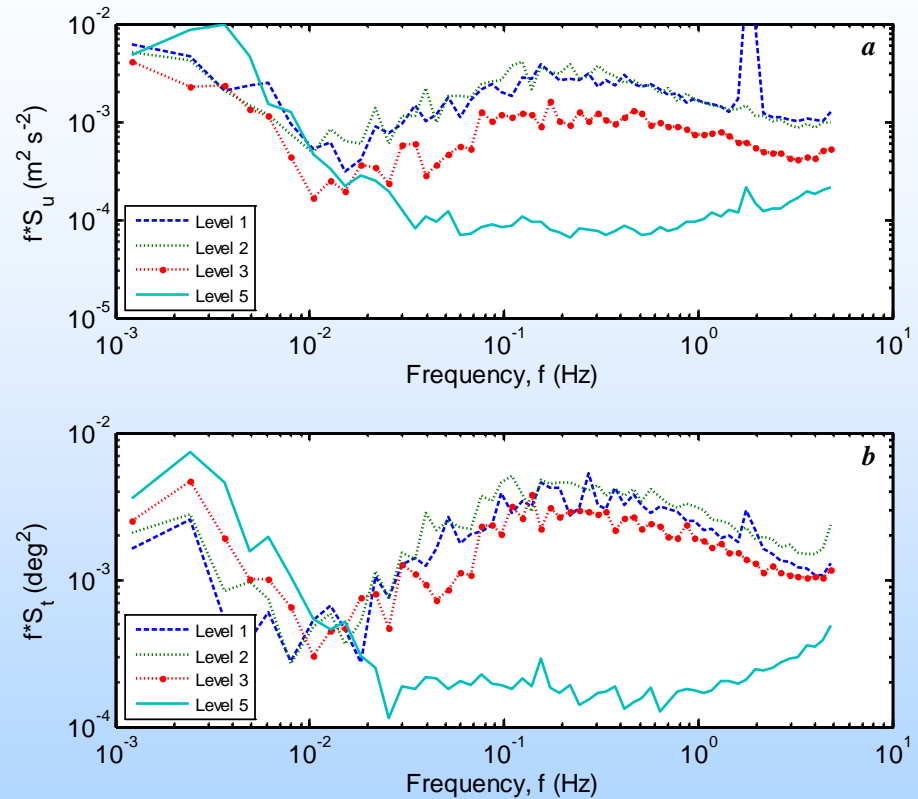
SHEBA

Typical Turbulent Spectra

for weakly and moderate stable (left) and very stable (right) conditions



Typical raw spectra of (a) the longitudinal wind component and (b) the sonic temperature at four levels (level 3 is missing) for weakly and moderate stable conditions during 14 February 1998 UTC (1998 YD 45.4167). Stability parameter increases with increasing height from 0.128 to 1.893, (levels 1, 2, 4, and 5). The bulk Richardson number also increases with increasing height from 0.0120 to 0.0734 but it is still below its critical value 0.2.



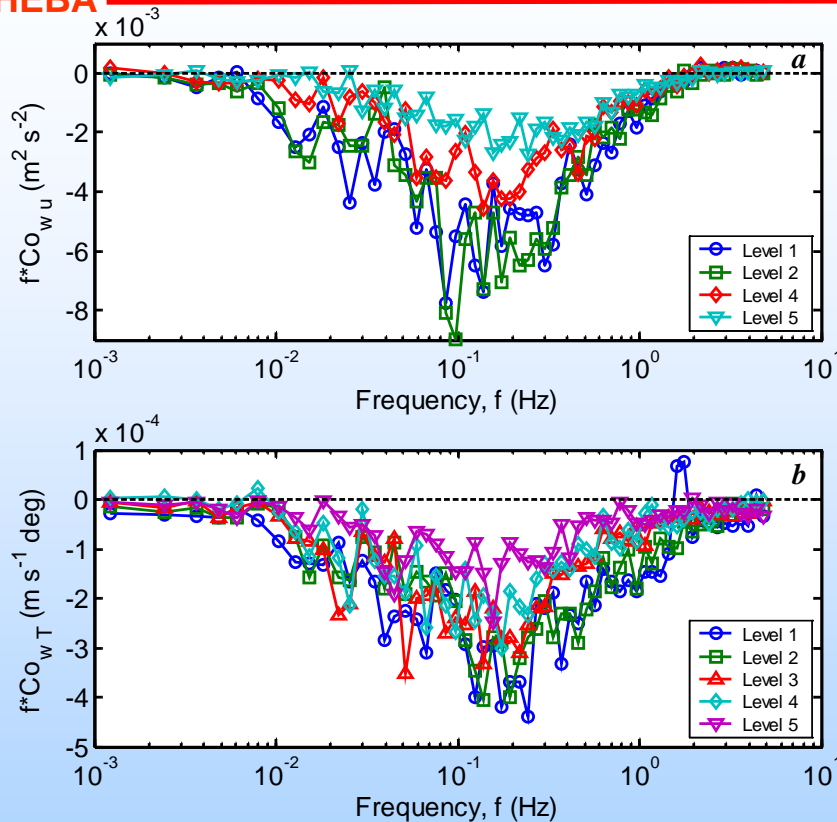
Typical raw spectra of (a) the longitudinal wind component and (b) the sonic temperature at four levels (level 4 is missing) for very strong stable conditions during 21 December 1997 UTC (1997 YD 355.00). For data presented here the stability parameters at levels 2, 3, and 5 are 3, 10.5, and 116.3 (sensible heat flux is missing for level 1). The bulk Richardson numbers at four levels are $Ri_{B1} = 0.0736$, $Ri_{B2} = 0.0839$, $Ri_{B3} = 0.1090$, and $Ri_{B5} = 0.2793$.



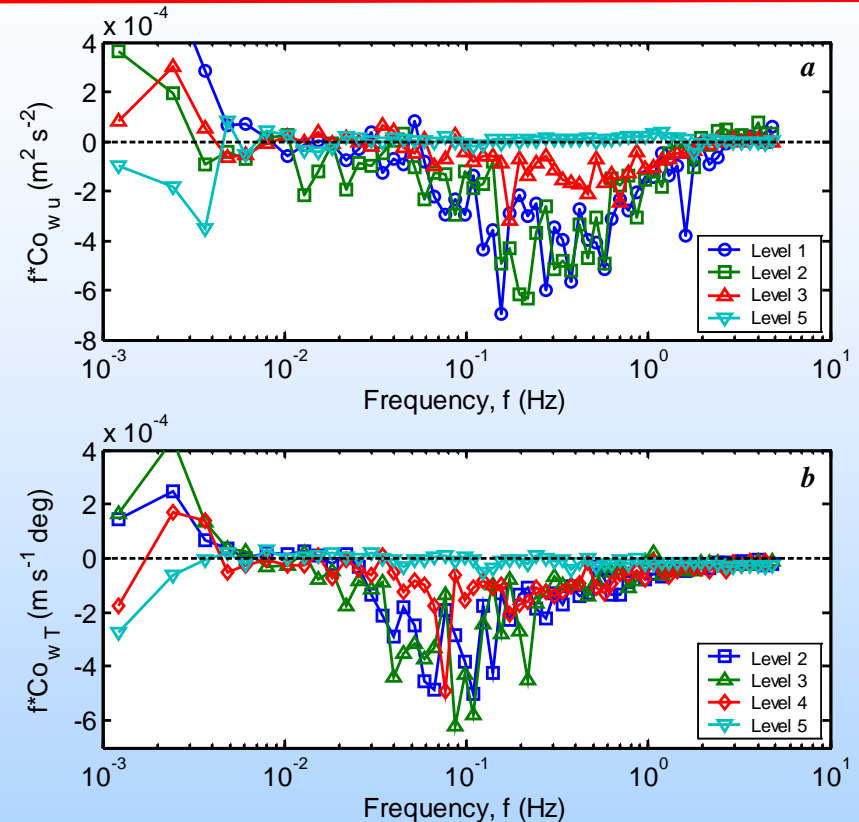
SHEBA

Typical Turbulent Cospectra

for weakly and moderate stable (left) and very stable (right) conditions



Typical (a) stress cospectra (1998 JD 45.4167), and cospectra of the sonic temperature flux (1997 JD 324.5833) for weakly and moderate stable conditions. In (a) u_* decreases with increasing height from 0.134 to 0.08 m/s. Stability parameter increases with increasing height from 0.128 to 1.893. In (b) downward sensible heat flux decreases with increasing height from -1.66 to -0.64 W/m² (level 1 to level 5). Stability parameter increases with increasing height from 0.096 to 0.533.



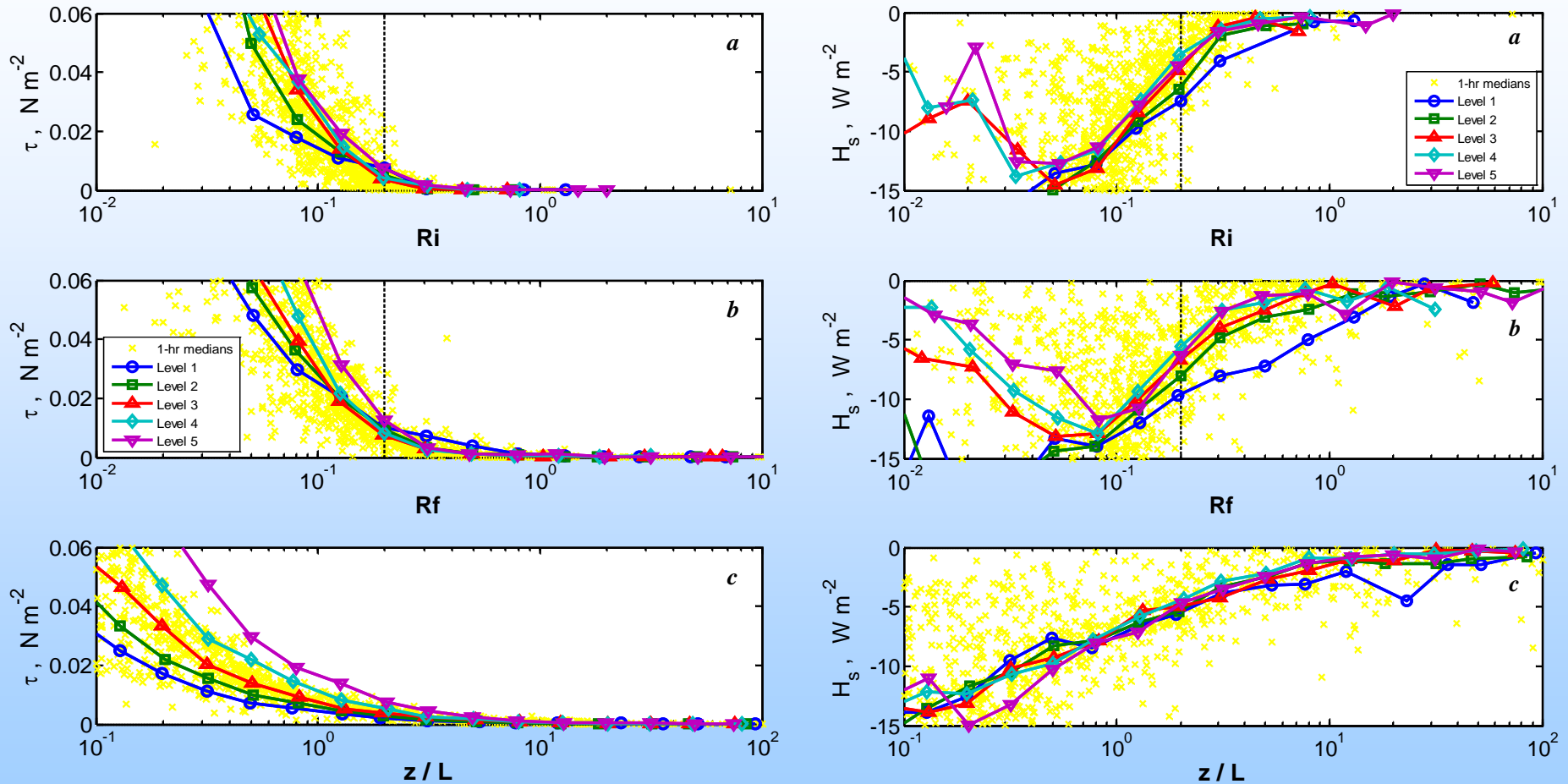
Typical cospectra of (a) the momentum flux (JD 355.00, 21 Dec., 1997), and (b) the sonic temperature flux (JD 507.75, 22 May, 1998) in the very stable regime. In (a) the stability parameter is 3 (level 2) and 10.5 (level 3). In (b) the stability parameters increase with increasing height: 1.41, 2.05, 6.34, 8.13 (levels 2–5).



SHEBA

Turbulence decay in the SBL

The critical Richardson number



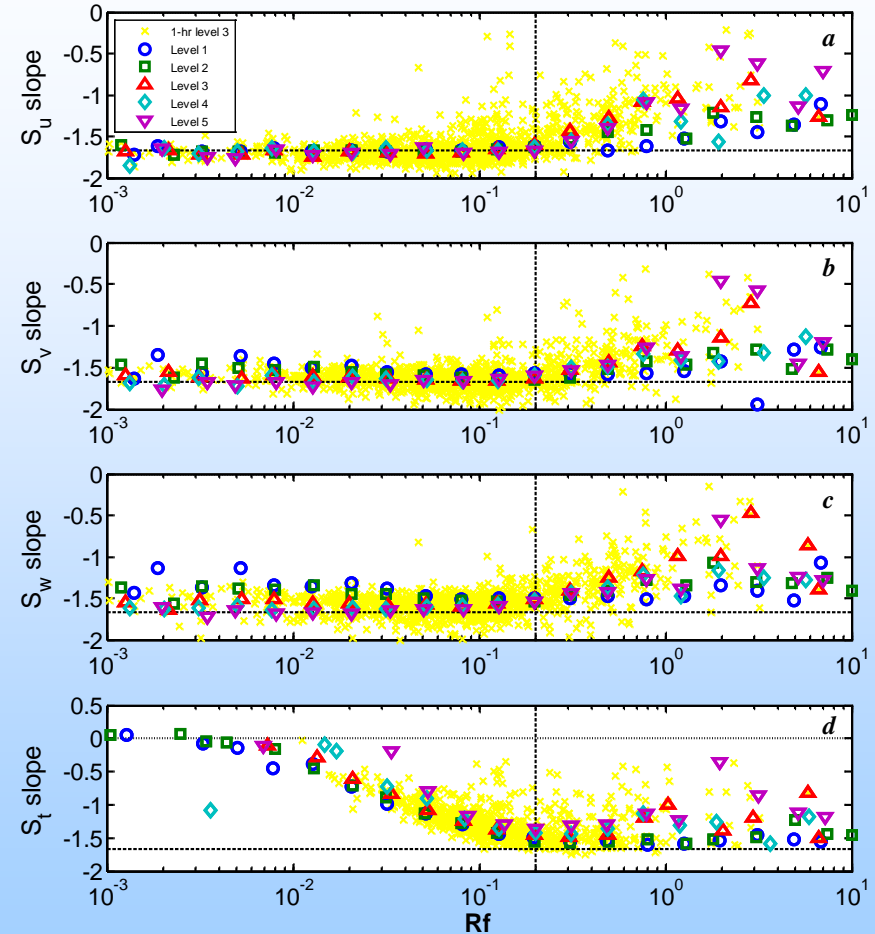
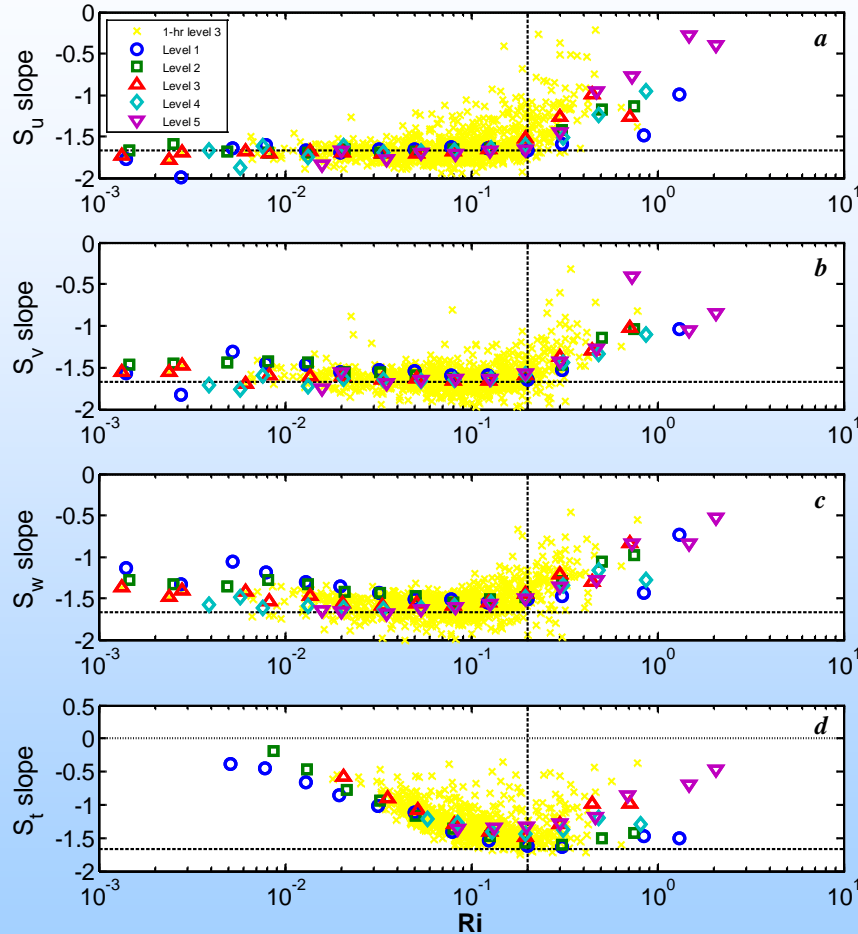
Behavior of the bin-averaged downward momentum flux (left panels) and for the sensible heat flux (right panels) for five levels of the main SHEBA tower plotted versus (a) Ri , (b) Rf , and (c) $\zeta = z/L$. Individual 1-hour averaged SHEBA data based on the median fluxes for the five levels are shown as the background x-symbols. The vertical dashed lines correspond to Ri and $Rf = 0.2$.



SHEBA

Turbulence decay in the SBL

Spectral slope in the inertial subrange



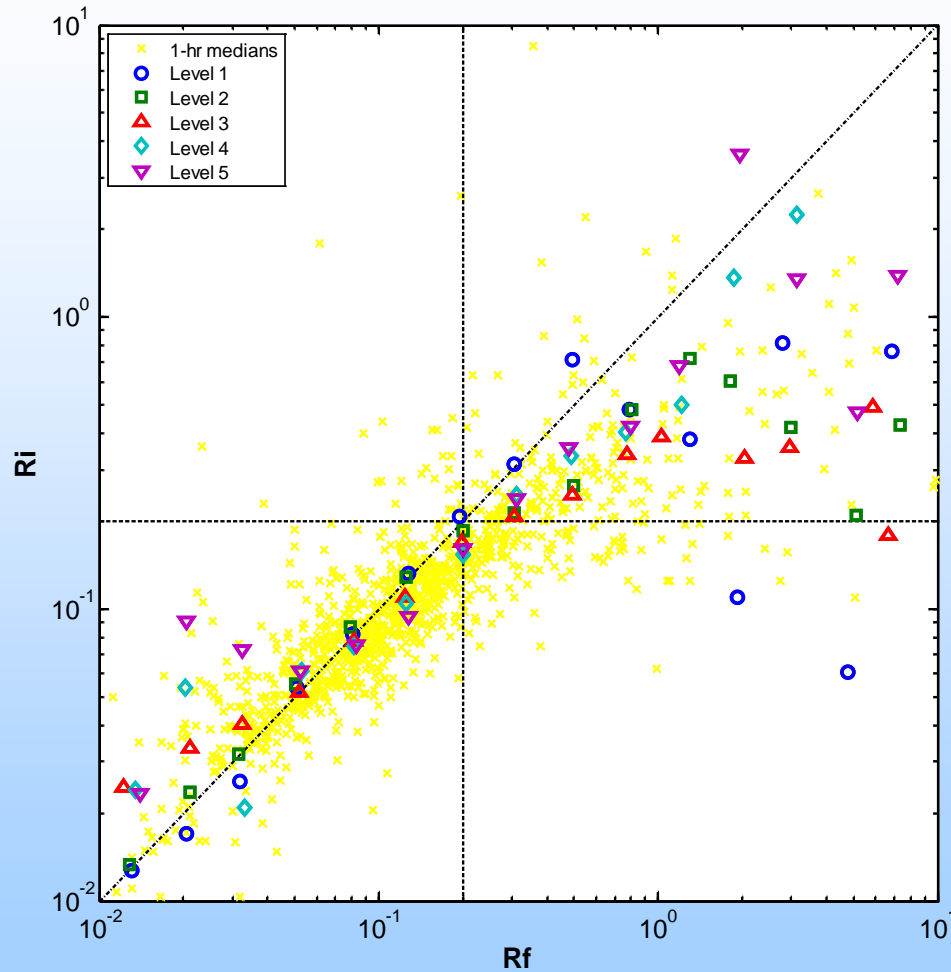
Plots of the bin-averaged spectral slope in the inertial subrange for the spectrum of the (a) longitudinal, (b) lateral, and (c) vertical velocity components and (d) the sonic temperature for five levels versus Ri (left panels) and Rf (right panels). The spectral slopes were computed in the 0.96-2.95 Hz frequency band. Individual 1-hour averaged data for level 3 are shown as the background x-symbols. The vertical dashed lines correspond to Ri & $Rf = 0.2$. The horizontal dashed lines represent the $-5/3$ Kolmogorov power law.



SHEBA

$$Ri < Ri_{cr} \text{ \& } Rf < Rf_{cr} \text{ (} Ri_{cr}=Rf_{cr}=0.20-0.25 \text{)}$$

Upper limit of applicability of the -5/3 Kolmogorov power-law



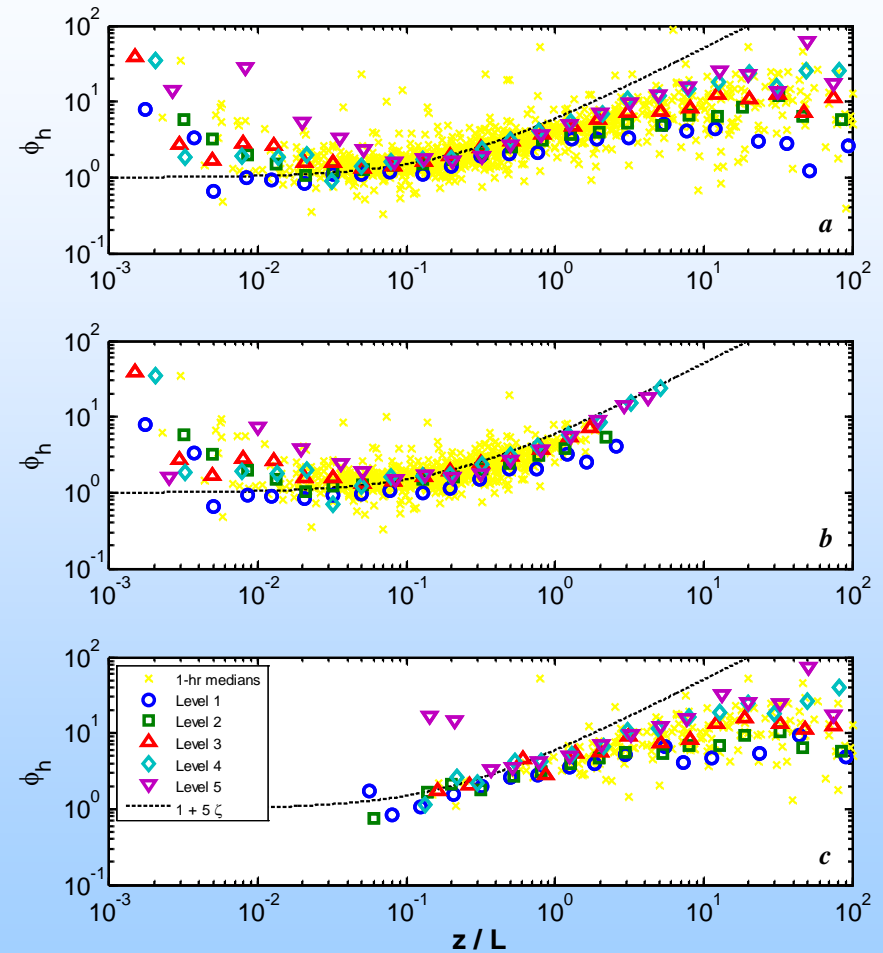
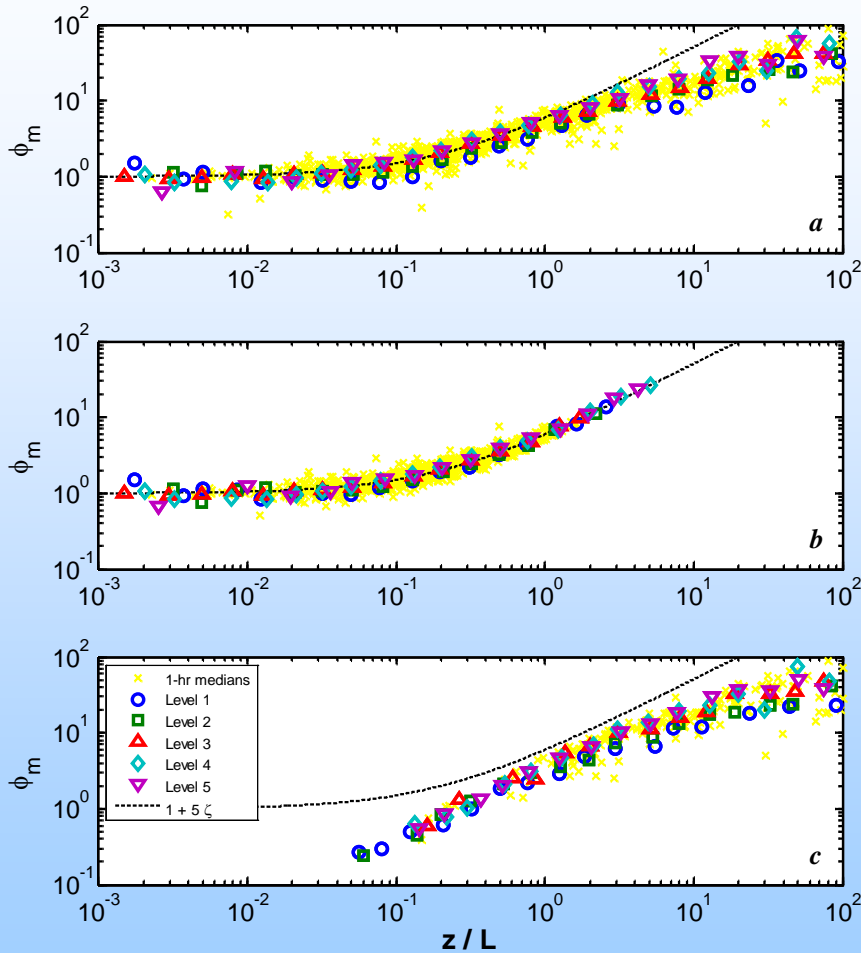
Bin-averaged gradient Richardson number (bin medians) plotted versus the flux Richardson number for the five levels of the main SHEBA tower during the 11 months of measurements plotted. The vertical and horizontal dashed lines correspond to Rf and $Ri = 0.2$, respectively. The dashed-dotted line is 1:1.



SHEBA

Back to “Kansas”

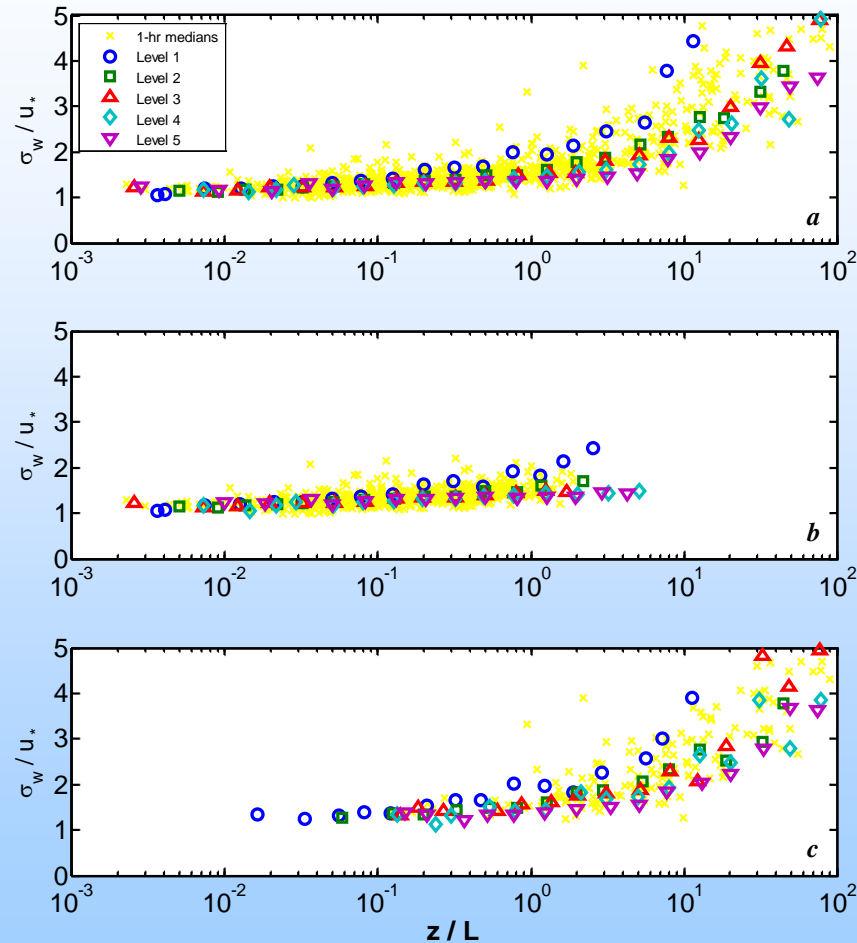
Return to z-less concept (ϕ_m & ϕ_h)



The bin-averaged ϕ_m (left panels) and ϕ_h (right panels) for five levels of the main SHEBA tower plotted versus $\zeta = z/L$ (a) for the original data, (b) in the subcritical regime when prerequisites $Ri < Ri_{cr}$ and $Rf < Rf_{cr}$ with $Ri_{cr} = Rf_{cr} = 0.2$ have been imposed on the data, and (c) in the supercritical regime when a prerequisites $Ri > Ri_{cr}$ and $Rf > Rf_{cr}$ have been imposed on the data.

Back to “Kansas”

Return to z -less concept (σ_w / u_*)



The bin-averaged σ_w / u_* for five levels of the main SHEBA tower plotted versus $\zeta = z/L$ (a) for the original data, (b) in the subcritical regime when prerequisites $Ri < Ri_{cr}$ and $Rf < Rf_{cr}$ with $Ri_{cr} = Rf_{cr} = 0.2$ have been imposed on the data, and (c) in the supercritical regime when a prerequisites $Ri > Ri_{cr}$ and $Rf > Rf_{cr}$ have been imposed on the data.

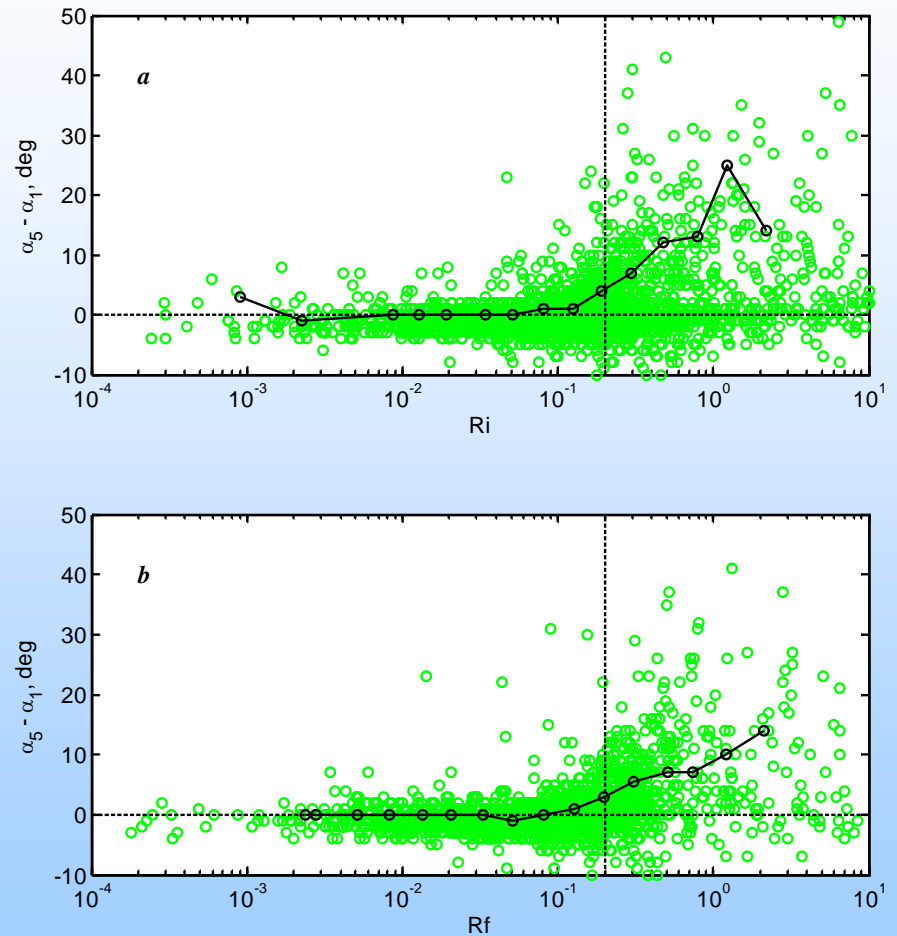
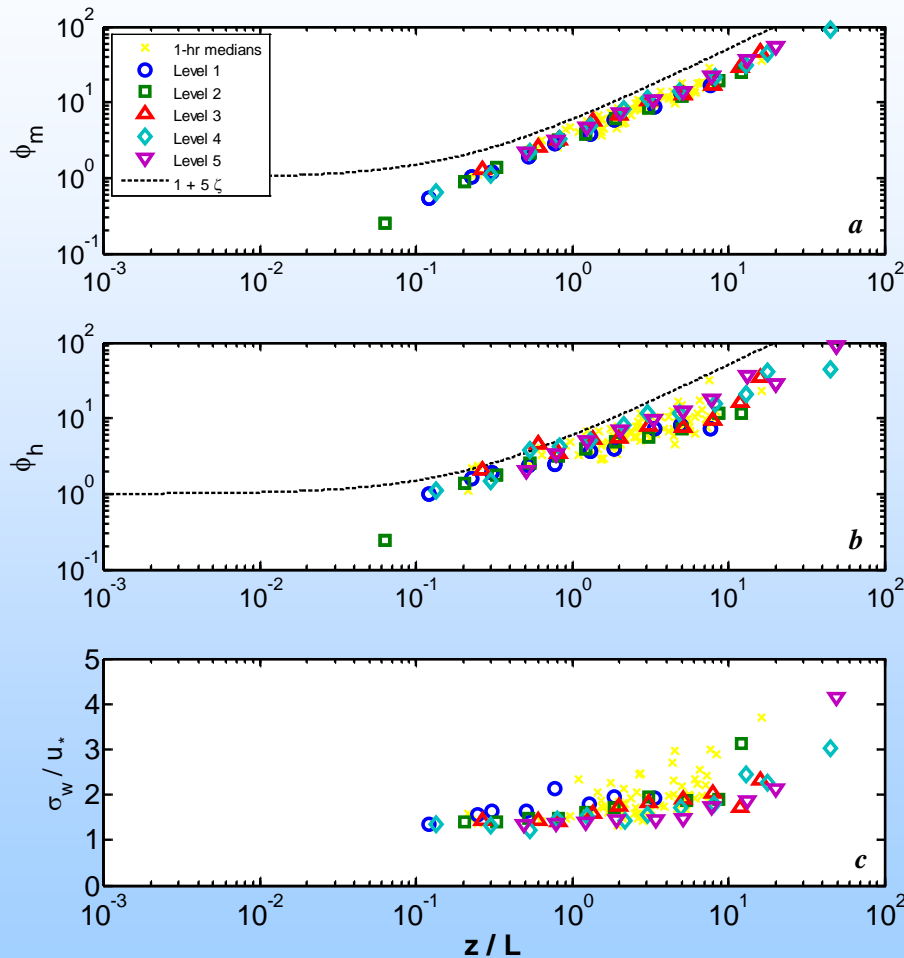


SHEBA

“Supercritical turbulence”

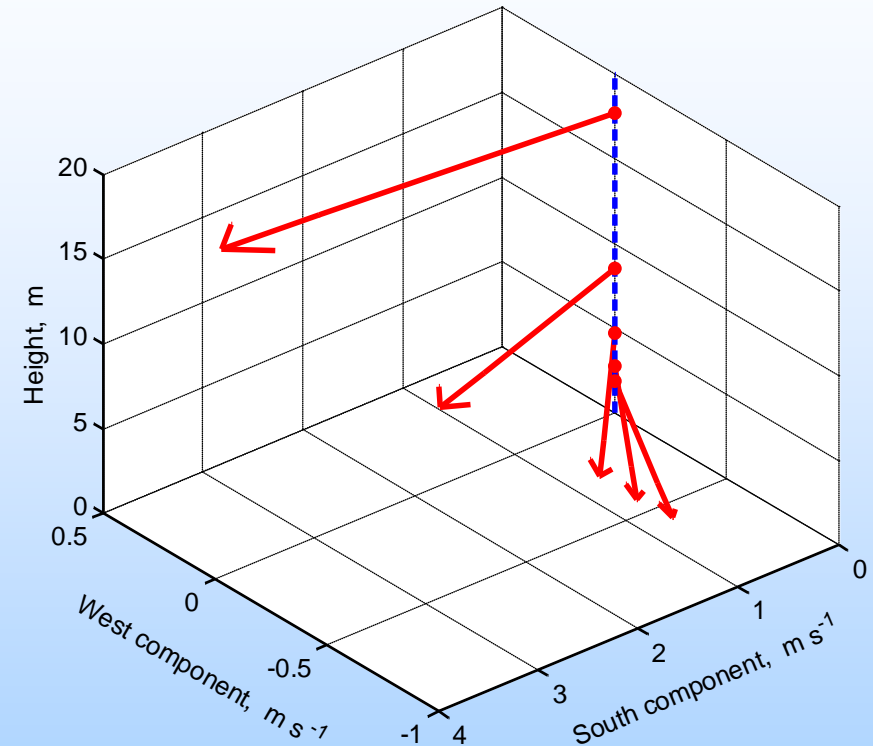
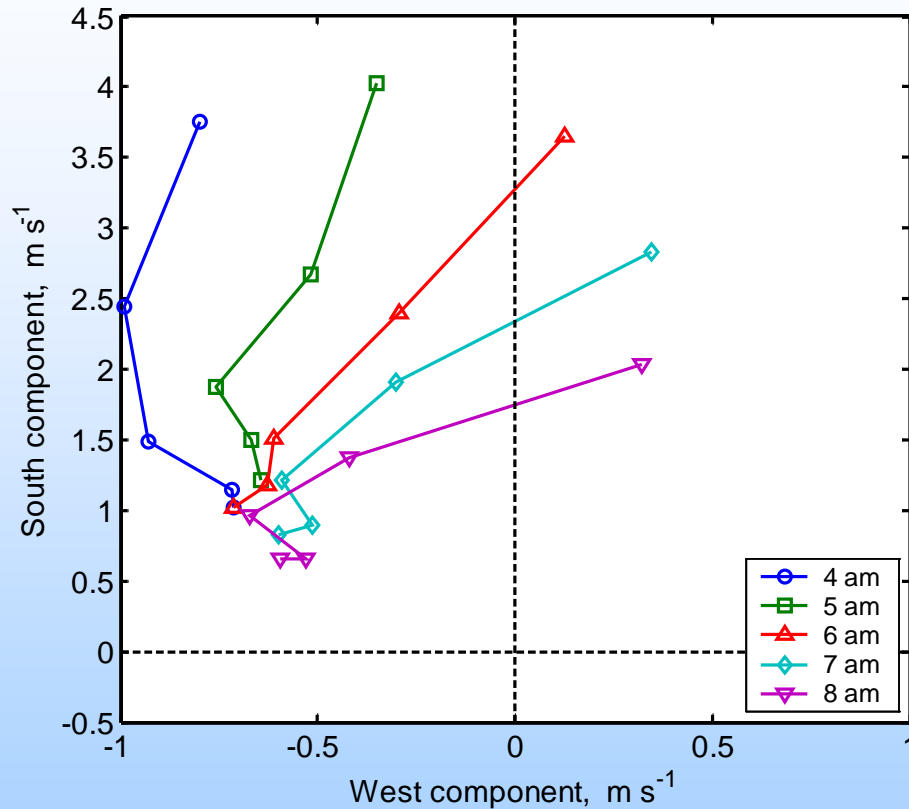
Turbulence without Richardson–Kolmogorov cascade

(Mazellier & Vassilicos (2010) *Phys. Fluids*. 22: 075101.)



The bin-averaged (a) ϕ_m , (b) ϕ_h , (c) σ_w/u_* (left panels) for five levels of the main SHEBA tower plotted versus $\zeta = z/L$ in the supercritical regime when prerequisites $0.2 < Ri < 0.5$ and $0.2 < Rf < 0.5$ have been imposed on the data. Difference between wind direction at levels 5 and 1 (right panels) as function of (a) Ri (at level 5) and (b) Rf (at level 5).

Ekman Layer



Evolving Ekman-type spirals during the polar day observed during JD 507 (22 May, 1998) for five hours from 12.00 to 16.00 UTC (4:00–8:00 a.m. local time, see the legend). Markers indicate ends of wind vectors at levels 1 to 5 (1.9, 2.7, 4.7, 8.6, and 17.7 m).

3D view of the Ekman spiral for 14:00 UTC JD 507 (local time 6 a.m.), 22 May 1998

Grachev et al. (2005), *Boundary-Layer Meteorology*, **116**(2), 201-235.



SHEBA

Conclusions



- Based on spectral analysis of wind velocity and air temperature fluctuations, it is shown that when both gradient Richardson number, Ri , and flux Richardson number, Rf , exceed a 'critical value' about 0.20-0.25, the inertial subrange associated with the Kolmogorov cascade dies out and vertical turbulent fluxes become small;
- However, some small-scale turbulence survives even in the supercritical regime, but this is non-Kolmogorov turbulence and it decays rapidly with further increasing stability;
- Similarity theory is based on the turbulent fluxes in the high-frequency part of the spectra that are associated with energy-containing/flux-carrying eddies. Spectral densities in this high-frequency band diminish as the Kolmogorov energy cascade weakens;
- Thus, according to our data, applicability of local Monin-Obukhov similarity theory in the stable conditions is limited by inequalities $Ri < Ri_{cr}$ and $Rf < Rf_{cr}$; with Ri_{cr} and $Rf_{cr} = 0.20-0.25$;
- However, it is found that $Rf_{cr} = 0.20-0.25$ is a primary threshold for applicability;
- Applying this prerequisite shows that the data follow classical Monin-Obukhov local z -less predictions after the irrelevant cases (non-Kolmogorov turbulence) have been filtered out.

Questions?

